CLOSED-FORM CRAMER-RAO LOWER BOUNDS FOR DOA ESTIMATION FROM TURBO-CODED SQUARE-QAM-MODULATED TRANSMISSIONS

Faouzi Bellili, Chaima Elguet, Souheib Ben Amor, Sofiène Affes, and Alex Stéphenne

INRS-EMT, 6900-800 de la Gauchetiere Ouest, Montreal (Qc), Canada, H5A 1K6.

{bellili, chaima.elguet, souheib.ben.amor, affes}@emt.inrs.ca and stephenne@ieee.org

ABSTRACT

This paper tackles the problem of the direction of arrival (DOA) estimation in turbo-coded systems. We derive for the first time the closed-form expressions for the Cramér-Rao lower bounds (CRLBs) of the code-aided (CA) DOA estimates from arbitrary square-QAM modulated signals. We succeed in factorizing the likelihood function of the system into two analogous terms linearizing thereby all the derivation steps of the Fisher information (FI) element. Simulation results demonstrate that the CRLB for the CA DOA estimates lies between its counterparts in non-data-aided (NDA) and data-aided (DA) estimation schemes. Moreover, the DOA CA CRLB improves by decreasing the coding rate highlighting thereby the potential gain in estimation performance stemming from the proper exploitation of the decoder output.

Index Terms— Direction of arrival (DOA), code-aided (CA), Cramér-Rao lower bound (CRLB), square-QAM modulations, turbo codes.

1. INTRODUCTION

The need for DOA estimation arises not only in broadband wireless communications but also in many other engineering applications including radar, sonar and emergency assistance devices [1]. Depending on the *a priori* knowledge about the transmitted symbols, DOA estimators can be broadly divided into two categories: DA and NDA methods. NDA approaches are *completely* blind and, as such, suffer from severe performance degradations at low signal-to-noise ratios (SNRs) and/or small number of snapshots. DA methods require the *complete* knowledge of the transmitted sequence thereby impinging on the whole throughput of the system. CA estimation, however, lies between these two extreme cases although it also assumes no *a priori* knowledge about the transmitted symbols. Rather, it exploits the *soft* information (about the transmitted bits) that is provided at each turbo iteration (see [2-9] and references therein), enhancing thereby the estimation performance while being spectrally efficient.

Turbo codes, in particular, have gained considerable attention since they were first introduced in [10] and are now being adopted in current- and future-generation wireless communication standards such as long-term evolution (LTE), LTE-advanced (LTE-A), and beyond (LTE-B) [11]. Although the research efforts on DOA estimation have, so far, mainly focused on the NDA scenario, we show in this contribution that substantial performance improvements can be achieved in CA estimation schemes. These improvements are highlighted through the derivation of the corresponding CA CRLB which is a practical lower bound that reflects the best achievable estimation performance theoretically [14]. We consider square-QAM-modulated signals which are also a key feature of current- and future-generation high-data-rates communication systems. It is worth mentioning here that the CRLBs of DOA estimates from linearly-modulated signals have been recently derived in [12, 13], but in the DA and NDA scenarios only. The new closed-form CA CRLBs are validated by another *empirical* approach that requires exhaustive Monte-Carlo simulations. The latter is borrowed from [16] that evaluates the CA CRLB of the time delay estimation problem.

This paper is organized as follows. In Section 2, we introduce the system model. In Section 3, we derive the analytical expressions for the considered DOA CA CRLB. In Section 4, we discuss the simulation results before drawing out some concluding remarks in Section 5.

Some of the common notations will be used throughout this paper. In fact, $\{.\}^T$ and $\{.\}^H$ denote the transpose and the Hermitian operators, respectively. The operators $\Re\{.\}$, $\Im\{.\}$ and $\{.\}^*$ return the real, imaginary parts and the conjugate of any complex quantity, respectively, whereas $|.|$ returns its amplitude. Moreover, j is the pure complex number that verifies $j^2 = -1$ and $\mathrm{E}\{.\}$ stands for the statistical expectation.

2. SYSTEM MODEL

A binary sequence of information bits is turbo encoded with coding rate R. The encoded bits are then scrambled with an outer interleaver and mapped onto a given Gray-coded (GC) constellation. The transmitted signal impinges on an array of N_a receiving antenna elements. At the output of the matched filter, the k^{th} recorded snapshot, $\mathbf{y}(k) = [y_1(k), y_2(k), \cdots, y_{N_a}(k)]^T$, is modeled as follows:

$$\mathbf{y}(k) = S\mathbf{a}(\phi)x(k) + \mathbf{w}(k), \quad k = 0, 1, \ldots, K-1, \tag{1}$$

where S is the channel coefficient and $\mathbf{a}(\phi)$ is the steering vector of the antennae array which is a function of the unknown DOA, ϕ, to be estimated. The additive white Gaussian noise (AWGN) components, $\mathbf{w}(k)$, are assumed spatially white, i.e., with covariance matrix $\mathrm{E}\{\mathbf{w}(k)\mathbf{w}(k)^H\} = \sigma^2\mathbf{I}$. They are also independent between snapshots. The transmitted symbols $\{x(k)\}_k$ are drawn from any M-ary GC square-QAM constellation. By *square* QAM we mean that $M = 2^{2p}$ $\big($i.e., QPSK, $16-$QAM, $64-$QAM, etc...$\big)$. We also assume that the energy of the transmitted symbols is normalized to one $\big($i.e., $\mathrm{E}\{|x(k)|^2\} = 1\big)$ so that the average SNR of the system is given by $\rho = \mathrm{E}\left\{S^2|x(k)|^2\right\}/\sigma^2 = S^2/\sigma^2$. The CRLB is a practical lower bound on the variance of any unbiased estimator $\widehat{\phi}$ of ϕ [14], i.e., it verifies $\mathrm{E}\left\{(\widehat{\phi} - \phi)^2\right\} \geq \mathrm{CRLB}(\phi)$. It is defined as:

$$\mathrm{CRLB}(\phi) \triangleq \frac{1}{I(\phi)}, \tag{2}$$

where $I(\phi)$ is the so-called Fisher information for the received data that is given by:

$$I(\phi) \triangleq -\mathrm{E}\left\{\frac{\partial^2 \mathcal{L}(\mathbf{Y};\phi)}{\partial \phi^2}\right\}. \tag{3}$$

In (3), $\mathbf{Y}$ is a matrix that gathers all the recorded snapshots and $\mathcal{L}(\mathbf{Y};\phi) \triangleq \ln\left(p[\mathbf{Y};\phi]\right)$ is the log-likelihood function (LLF) $\big(p[\mathbf{Y};\phi]$ being the pdf of $\mathbf{Y}$ parameterized by $\phi\big)$.

3. DERIVATION OF THE CLOSED-FORM EXPRESSIONS FOR THE DOA CA CRLB

Since the transmitted symbols are some *soft* representations for different blocks of the coded bits and as the latter are assumed to be statistically independent (due to the large-size interleaver) [3, 4], the transmitted symbols are also independent. Therefore, $p[\mathbf{Y};\phi]$ is factorized as follows:

$$p[\mathbf{Y};\phi] = \prod_{k=0}^{K-1} p[\mathbf{y}(k);\phi], \tag{4}$$

where $p[\mathbf{y}(k);\phi]$ is the pdf of the k^{th} snapshot, $\mathbf{y}(k)$, parameterized by ϕ. Using the fact that $\|\mathbf{a}(\phi)\|^2 = N_a$, it can be shown from (1) that:

$$p[\mathbf{y}(k);\phi] = \frac{1}{\pi^{N_a}\sigma^{N_a}} \exp\!\big(-\tfrac{1}{\sigma^2}\|\mathbf{y}(k)\|^2\big)\, D_k(\phi), \tag{5}$$

in which the term $D_k(\phi)$ is given by:

$$D_k(\phi) \;=\; \sum_{c_m\in\mathcal{C}_p} Pr[x(k)=c_m] \exp\left(-\tfrac{N_a S^2 |c_m|^2}{\sigma^2}\right) \times \exp\left(\tfrac{2}{\sigma^2}\Re\left\{c_m^* S\,\mathbf{a}(\phi)^H\mathbf{y}(k)\right\}\right). \tag{6}$$

In (6), $\mathcal{C}_p = \{c_1, c_2, \ldots, c_M\}$ is the alphabet of the GC $2^{2p}-$QAM constellation and $\left\{Pr[x(k)=c_m]\right\}_m$ are the *a priori* probabilities (APPs) of the transmitted symbols that will be established in the next subsection.

3.1. Derivation of the symbols' APPs

Consider a M-ary GC square-QAM constellation where each alphabet's point, c_m, is mapped onto a unique sequence of $\log_2(M) = 2p$ bits according to the following notation: $c_m \longleftrightarrow \bar{b}_1^m\bar{b}_2^m\cdots\bar{b}_l^m\cdots\bar{b}_{2p}^m$. Likewise, we use $x(k) \longleftrightarrow b_1^k b_2^k\cdots b_l^k\cdots b_{2p}^k$ to denote the bit sequence conveyed by the k^{th} transmitted symbol $x(k)$. Again, due to the independence of the code bits [3, 4], the APPs of each transmitted symbol factorize as follows:

$$Pr[x(k)=c_m] = \prod_{l=1}^{2p} Pr\left[b_l^k = \bar{b}_l^m\right], \qquad \forall c_m\in\mathcal{C}_p. \tag{7}$$

We also define the LLR of the l^{th} coded bit, b_l^k, that is conveyed by transmitting the symbol $x(k)$ as follows:

$$L_l(k) \triangleq \ln\left(\frac{Pr[b_l^k=1]}{Pr[b_l^k=0]}\right). \tag{8}$$

Using (8) and the fact that $Pr[b_l^k=0] + Pr[b_l^k=1] = 1$, one can straightforwardly obtain the following generic expression:

$$Pr[b_l^k = \bar{b}_l^m] = \frac{1}{2\cosh\big(L_l(k)/2\big)}\, e^{(\bar{b}_l^m-1)\frac{L_l(k)}{2}}, \tag{9}$$

in which the bit $\bar{b}_l^m$ is either 0 or 1 depending on which of the symbols, $\{c_m\}_m$, is drawn at time instant k, and of course on the underlying Gray mapping. Hence, injecting (9) in (7) we obtain:

$$Pr[x(k)=c_m] = \underbrace{\prod_{l=1}^{2p}\frac{1}{2\cosh\big(L_l(k)/2\big)}}_{\beta_k}\prod_{l=1}^{2p} e^{(\bar{b}_l^m-1)\frac{L_l(k)}{2}}. \tag{10}$$

In the sequel, we will rewrite the APPs in (10) in a more convenient form that allows the factorization of $D_k(\phi)$ given in (6). To that end, we describe a simple recursive process that allows the construction of a GC $2^{2p}-$QAM starting from any given GC $2^{2(p-1)}-$QAM and using any *basic* GC QPSK:

- *step 1*: build the top-right quadrant (denoted from now on as $\widetilde{\mathcal{C}}_p$) of the desired $2^{2p}-$QAM from all the points[1] of the available $2^{2(p-1)}-$QAM constellation. For the sake of clarity and without loss of generality, we assume that the two missing bits of the new quadrant always occupy the two least significant positions.
- *step 2*: build the three remaining empty quadrants of the desired $2^{2p}-$QAM by symmetries with respect to the $x-$axis, the $y-$axis, and the center point, respectively. In light of "*step 1*", all the points of the desired constellation are inherently missing 2 bits each which will be added in the next step.
- *step 3*: copy the two bits of each quadrant in the basic GC QPSK constellation to all the points that belong to the same quadrant in the incomplete $2^{2p}-$QAM constellation obtained in "*step 2*".

As an example, we illustrate in Fig. 1 the recursive construction of a GC $16-$QAM constellation from a $4-$QAM GC one.

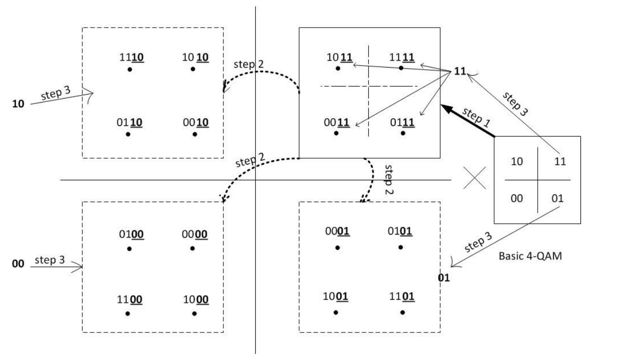

Fig. 1. Recursive construction of GC square-QAM constellations illustrated here from $4-$QAM to $16-$QAM.

In this work, for clarity reasons but with no loss of generality, we will build on the basic QPSK depicted in Fig. 1 and use it in all subsequent construction iterations. In light of the three symmetries in "*step 2*", each four symmetrical points $\tilde{c}_m, \tilde{c}_m^*, -\tilde{c}_m$ and $-\tilde{c}_m^*$ (for any $\tilde{c}_m$ in $\widetilde{\mathcal{C}}_p$) have the same $2p-2$ most significant bits, $\bar{b}_1^m\bar{b}_2^m\bar{b}_3^m\ldots\bar{b}_{2p-3}^m\bar{b}_{2p-2}^m$, which we use to define the following quantity:

$$\mu_{k,p}(c_m) \triangleq \prod_{l=1}^{2p-2} e^{(2\bar{b}_l^m-1)\frac{L_l(k)}{2}}, \quad \forall\, c_m\in\mathcal{C}_p, \tag{11}$$

that verifies $\mu_{k,p}(\tilde{c}_m) = \mu_{k,p}(-\tilde{c}_m) = \mu_{k,p}(\tilde{c}_m^*) = \mu_{k,p}(-\tilde{c}_m^*)$, $\forall\, \tilde{c}_m$ in $\widetilde{\mathcal{C}}_p$. Then, by using this result back in (10), the symbol's APPs are obtained as follows for any $\tilde{c}_m\in\widetilde{\mathcal{C}}_p$:

$$Pr[x(k)\!=\!\tilde{c}_m] = \beta_k\,\mu_{k,p}(\tilde{c}_m)\, e^{-\frac{L_{2p-1}(k)}{2}} e^{\frac{L_{2p}(k)}{2}}, \tag{12}$$

$$Pr[x(k)\!=\!\tilde{c}_m^*] = \beta_k\,\mu_{k,p}(\tilde{c}_m)\, e^{\frac{L_{2p-1}(k)}{2}} e^{\frac{L_{2p}(k)}{2}}, \tag{13}$$

$$Pr[x(k)\!=\!-\tilde{c}_m] = \beta_k\,\mu_{k,p}(\tilde{c}_m)\, e^{\frac{L_{2p-1}(k)}{2}} e^{-\frac{L_{2p}(k)}{2}}, \tag{14}$$

$$Pr[x(k)\!=\!-\tilde{c}_m^*] = \beta_k\,\mu_{k,p}(\tilde{c}_m)\, e^{-\frac{L_{2p-1}(k)}{2}} e^{-\frac{L_{2p}(k)}{2}}. \tag{15}$$

3.2. Factorization of $D_k(\phi)$:

Using the fact that $\mathcal{C}_p = \widetilde{\mathcal{C}}_p \cup (-\widetilde{\mathcal{C}}_p) \cup \widetilde{\mathcal{C}}_p^* \cup (-\widetilde{\mathcal{C}}_p^*)$ and plugging the expression of the symbol's APPs already established in (12) through (15) back into (6) and using the identity $e^x + e^{-x} = 2\cosh(x)$, we obtain the following result:

$$D_k(\phi) \;=\; 2\beta_k \sum_{\tilde{c}_m\in\tilde{\mathcal{C}}_p} \mu_{k,p}(\tilde{c}_m)\, e^{-\rho N_a|\tilde{c}_m|^2} \times \Bigg[\cosh\!\Big(\tfrac{2}{\sigma^2}\Re\left\{\tilde{c}_m^* S\mathbf{a}(\phi)^H\mathbf{y}(k)\right\} + \tfrac{L_{2p}(k)}{2} + \tfrac{L_{2p-1}(k)}{2}\Big) \times + \cosh\!\Big(\tfrac{2}{\sigma^2}\Re\left\{\tilde{c}_m S\mathbf{a}(\phi)^H\mathbf{y}(k)\right\} + \tfrac{L_{2p}(k)}{2} - \tfrac{L_{2p-1}(k)}{2}\Big)\Bigg]. \tag{16}$$

[1] The same points' layout in the original $2^{2(p-1)}-$QAM constellation is used, i.e., the constellation is placed as is in the new quadrant.

Then, using the identities $\cosh(x)+\cosh(y) = 2\cosh(\frac{x+y}{2})\cosh(\frac{x-y}{2})$, $\tilde{c}_m^* + \tilde{c}_m = 2\Re\{\tilde{c}_m\}$ and $\tilde{c}_m^* - \tilde{c}_m = -2j\Im\{\tilde{c}_m\}$, it follows that:

$$D_k(\phi) = 4\beta_k \sum_{\tilde{c}_m \in \tilde{\mathcal{C}}_p} \mu_{k,p}(\tilde{c}_m) e^{-\rho N_a |\tilde{c}_m|^2} \cosh\Big(\tfrac{2S\sqrt{N_a}\Re\{\tilde{c}_m\}}{\sigma^2} u_k(\phi) + \tfrac{L_{2p}(k)}{2}\Big) \times \cosh\Big(\tfrac{2S\sqrt{N_a}\Im\{\tilde{c}_m\}}{\sigma^2} v_k(\phi) + \tfrac{L_{2p-1}(k)}{2}\Big), \quad (17)$$

in which $u_k(\phi)$ and $v_k(\phi)$ are, respectively, the real and imaginary parts of the receive-beamforming output steered toward the unknown DOA to be estimated, i.e.:

$$u_k(\phi) \triangleq \tfrac{1}{\sqrt{N_a}} \Re\Big\{\mathbf{a}(\phi)^H \mathbf{y}(k)\Big\} \quad \text{and} \quad v_k(\phi) \triangleq \tfrac{1}{\sqrt{N_a}} \Im\Big\{\mathbf{a}(\phi)^H \mathbf{y}(k)\Big\}.$$

Since each $\tilde{c}_m \in \widetilde{C}_p$ can be written as $\tilde{c}_m = [2i-1]d_p + j[2n-1]d_p$ for some $1 \leq i, n \leq 2^{p-1}$, where $2d_p$ is the inter-symbol distance given in [12], we will from now on use the superscript (i,n) instead of m $\big[$i.e., $\tilde{c}_m \longleftrightarrow \bar{b}_1^{(i,n)}\bar{b}_2^{(i,n)}\cdots\bar{b}_{2p}^{(i,n)}\big]$. Further, by closely inspecting the recursive construction process, it can be easily shown that (see [17] and [18] for more details):

Assertion: the GC $2^{2p}-$QAM has the following property:

- The odd-position bits, $\bar{b}_{2l-1}^{(i,n)}$, do not change by scanning each *horizontal* line of the constellation points.
- The even-position bits, $\bar{b}_{2l}^{(i,n)}$, do not change by scanning each *vertical* line of the constellation points.

In a nutshell, the fact that the odd-position bits, $\{\bar{b}_{2l-1}^{(i,n)}\}_{l=1}^{p}$, do not change for each horizontal line means that they do not change by varying the symbols' abcissa, $[2i-1]d_p$, or equivalently by changing the counter i. Therefore, $\{\bar{b}_{2l-1}^{(i,n)}\}_{l=1}^{p}$ are function of n only and, by the same token, the even-position bits, $\{\bar{b}_{2l}^{(i,n)}\}_{l=1}^{p}$, are function of i only. As a consequence, we will from now on drop the vanishing counter from each group of bits and denote them simply as:

$$\Big\{\bar{b}_{2l-1}^{(i,n)} \equiv \bar{b}_{2l-1}^{(n)} \quad \text{and} \quad \bar{b}_{2l}^{(i,n)} \equiv \bar{b}_{2l}^{(i)}\Big\}_{l=1}^{p}. \quad (18)$$

Now, by using the result of (18) in (11) and grouping the odd-position (resp. even-position) bits together, we obtain the decomposition:

$$\mu_{k,p}(\tilde{c}_m) = \theta_{k,2p}(i)\theta_{k,2p-1}(n), \quad (19)$$

where $\theta_{k,2p}(i)$ and $\theta_{k,2p-1}(n)$ are given by:

$$\theta_{k,2p}(i) = \prod_{l=1}^{p-1} e^{(2\bar{b}_{2l}^{(i)}-1)\frac{L_{2l}(k)}{2}} \; ; \; \theta_{k,2p-1}(n) = \prod_{l=1}^{p-1} e^{(2\bar{b}_{2l-1}^{(n)}-1)\frac{L_{2l-1}(k)}{2}}.$$

Plugging (19) in (17) and using $\widetilde{\mathcal{C}}_p = \big\{[2i-1]d_p + j[2n-1]d_p\big\}_{i,n=1}^{2^{p-1}}$, we obtain the result given by (21) [shown on the top of the next page]. Finally, by splitting the two sums in (21), $D_k(\phi)$ factorizes as follows:

$$D_k(\phi) = 4\beta_k F_{k,2p}\big(u_k(\phi)\big) \times F_{k,2p-1}\big(v_k(\phi)\big), \quad (20)$$

where the function $F_{k,q}(.)$ is given by (for $q = 2p$ or $2p-1$):

$$F_{k,q}(x) = \sum_{i=1}^{2^{p-1}} \theta_{k,q}(i) e^{-\rho N_a d_p^2 [2i-1]^2} \cosh\Big(\tfrac{2S[2i-1]\sqrt{N_a}d_p}{\sigma^2} x + \tfrac{L_q(k)}{2}\Big).$$

Furthermore, by following the same reasoning of Appendix C in [12], it can be shown that:

$$p[u_k(\phi), v_k(\phi)] = p[\tfrac{1}{\sqrt{N_a}} \mathbf{a}(\phi)^H \mathbf{y}(k)] = p[u_k(\phi)]p[v_k(\phi)], \quad (22)$$

where the pdfs of the two *independent* random variables (RVs), $u_k(\phi)$ and $v_k(\phi)$, are given by:

$$p\big[u_k(\phi)\big] = \tfrac{2\beta_{k,2p}}{\sqrt{\pi\sigma^2}} F_{k,2p}\big(u_k(\phi)\big) e^{-\frac{u_k(\phi)^2}{\sigma^2}}, \quad (23)$$

$$p\big[v_k(\phi)\big] = \tfrac{2\beta_{k,2p-1}}{\sqrt{\pi\sigma^2}} F_{k,2p-1}\big(v_k(\phi)\big) e^{-\frac{v_k(\phi)^2}{\sigma^2}}. \quad (24)$$

3.3. Derivation of the closed-form DOA CA CRLB

By injecting (5) in (4), it follows that:

$$\mathcal{L}(\mathbf{Y};\phi) = -KN_a \ln\big(\pi\sigma^2\big) + \frac{1}{\sigma^2}\sum_{k=0}^{K-1}\big\|\mathbf{y}(k)\big\|^2 + \sum_{k=0}^{K-1}\ln\big(D_k(\phi)\big).$$

Then, using (20) and discarding the constant terms $\big($that do not depend on $\phi\big)$, it follows that the *useful* LLF is decomposed as the sum of two analogous terms as follows:

$$\mathcal{L}(\mathbf{Y};\phi) = \sum_{k=0}^{K-1}\ln\Big(F_{k,2p}\big(u_k(\phi)\big)\Big) + \sum_{k=0}^{K-1}\ln\Big(F_{k,2p-1}\big(v_k(\phi)\big)\Big). \quad (25)$$

By using (25) in (3) and owing to the linearity of the *derivative* and *expectation* operators, we obtain:

$$I(\phi) = \sum_{k=0}^{K-1}\Big[\gamma_{k,2p}(\phi) + \gamma_{k,2p-1}(\phi)\Big], \quad (26)$$

where $\gamma_{k,2p}(\phi) \triangleq -\mathrm{E}\left\{\partial^2 \ln\big(F_{k,2p}\big(u_k(\phi)\big)\big)/\partial\phi^2\right\}$ and $\gamma_{k,2p-1}(\phi) \triangleq -\mathrm{E}\left\{\partial^2 \ln\big(F_{k,2p-1}\big(v_k(\phi)\big)\big)/\partial\phi^2\right\}$. Next, we will only detail the derivation of $\gamma_{k,2p}(\phi)$ since $\gamma_{k,2p-1}(\phi)$ is obtained in the same way due to the apparent symmetries between the pdfs of $u_k(\phi)$ and $v_k(\phi)$ in (23) and (24). In fact, since $u_k(\phi)$ and $\dot{u}_k(\phi) = \frac{\partial u_k(\phi)}{\partial\phi}$ are two independent RVs, it follows that:

$$\gamma_{k,2p}(\phi) = \mathbb{E}\left\{\dot{u}_k^2(\phi)\right\}\left[\mathbb{E}\left\{\frac{F'^2_{k,2p}\big(u_k(\phi)\big)}{F^2_{k,2p}\big(u_k(\phi)\big)}\right\} - \mathbb{E}\left\{\frac{F''_{k,2p}\big(u_k(\phi)\big)}{F_{k,2p}\big(u_k(\phi)\big)}\right\}\right] - \mathbb{E}\left\{\ddot{u}_k(\phi)\frac{F'_{k,2p}\big(u_k(\phi)\big)}{F_{k,2p}\big(u_k(\phi)\big)}\right\}, \quad (27)$$

where $F'_{k,2p}(x)$ and $F''_{k,2p}(x)$ are the first and second derivatives of $F_{k,2p}(x)$ with respect to the working variable x. In order to derive the expectations involved in (27), we define beforehand the following two quantities (for $q = 2p$ or $2p-1$) that will appear repeatedly:

$$\omega_{k,q} \triangleq 2d_p^2\beta_{k,q}\cosh\left(\tfrac{L_q(k)}{2}\right)\sum_{i=1}^{2^{p-1}}\theta_{k,q}(i)[2i-1]^2,$$

$$\alpha_{k,q} \triangleq 2d_p\beta_{k,q}\sinh\left(\tfrac{L_q(k)}{2}\right)\sum_{i=1}^{2^{p-1}}\theta_{k,q}(i)[2i-1].$$

By integration over the pdf of $u_k(\phi)$ in (23) it follows that:

$$\mathbb{E}\left\{\frac{F''_{k,2p}\big(u_k(\phi)\big)}{F_{k,2p}\big(u_k(\phi)\big)}\right\} = \int_{\mathbb{R}}\frac{F''_{k,2p}\big(u_k(\phi)\big)}{F_{k,2p}\big(u_k(\phi)\big)}p[u_k(\phi)]\mathrm{d}u_k(\theta), = \tfrac{2\beta_{k,2p}}{\sqrt{\pi\sigma^2}}\int_{\mathbb{R}}F''_{k,2p}\big(u_k(\phi)\big)e^{\frac{-u_k^2(\phi)}{\sigma^2}}\mathrm{d}u_k(\phi). \quad (28)$$

After expanding the expression of $F''_{k,2p}(x)$ using the identity $\cosh(x+y) = \cosh(x)\cosh(y) + \sinh(x)\sinh(y)$ and making use of the following result (shown via "integration by parts"):

$$\int_0^{+\infty}\cosh\big(bx\big)e^{-ax^2}dx = \tfrac{1}{2}\sqrt{\tfrac{\pi}{a}}e^{\frac{b^2}{4a}}, \quad \forall a > 0 \text{ and } b \in \mathbb{R},$$

it follows that:

$$\mathbb{E}\left\{\frac{F''_{k,2p}\big(u_k(\phi)\big)}{F_{k,2p}\big(u_k(\phi)\big)}\right\} = \tfrac{4N_a}{\sigma^2}\rho\omega_{k,2p}. \quad (29)$$

Moreover, by following the same rationale of Appendix A in [12], it can be shown that $\dot{u}_k(\phi)$ is written as follows:

$$\dot{u}_k(\theta) = \tfrac{jS}{2\sqrt{N_a}}\dot{\mathbf{a}}(\theta)^H\mathbf{a}(\theta)\Im\left\{x(k)\right\} + \tfrac{1}{2\sqrt{N_a}}\Re\Big\{\dot{\mathbf{a}}(\theta)^H\mathbf{w}(k)\Big\}.$$

After some tedious algebra, the closed-form expression of $\mathbb{E}\left\{\dot{u}_k(\theta)^2\right\}$ is obtained as follows (cf. Appendix A of [12] for some hints):

$$\mathbb{E}\left\{\dot{u}_k(\phi)^2\right\} = \tfrac{\sigma^2}{2N_a}\big\|\dot{\mathbf{a}}(\phi)\big\|^2 + \tfrac{S^2}{2N_a}\big|\mathbf{a}(\phi)^H\dot{\mathbf{a}}(\phi)\big|^2\left(1 - \frac{\omega_{k,2p-1}}{2}\right).$$

$$D_k(\phi) = 4\beta_k \sum_{i=1}^{2^{p-1}} \sum_{n=1}^{2^{p-1}} \Big[\theta_{k,2p}(i) e^{-\rho N_a d_p^2 [2i-1]^2} \cosh\Big(\tfrac{2S[2i-1]\sqrt{N_a} d_p}{\sigma^2} u_k(\phi) + \tfrac{L_{2p}(k)}{2}\Big) \times \theta_{k,2p-1}(n) e^{-\rho N_a d_p^2 [2n-1]^2} \cosh\Big(\tfrac{2S[2n-1]\sqrt{N_a} d_p}{\sigma^2} v_k(\phi) + \tfrac{L_{2p-1}(k)}{2}\Big)\Big]. \quad (21)$$

After tedious algebraic manipulations, we also obtain the closed-form expressions for the remaining expectations involved in (27) as follows (cf. [12] for some hints):

$$\mathbb{E}\left\{\frac{F'^2_{k,2p}\big(u_k(\phi)\big)}{F^2_{k,2p}\big(u_k(\phi)\big)}\right\} = \tfrac{4N_a}{\sigma^2}\rho\nu_{k,2p}(\rho), \quad (30)$$

$$\mathbb{E}\Big\{\ddot{u}(k)\frac{F'_{k,2p}\big(u_k(\phi)\big)}{F_{k,2p}\big(u_k(\phi)\big)}\Big\} = -2\big\|\dot{\mathbf{a}}(\phi)\big\|^2\rho\,\omega_{k,2p} -2\Im\left\{\mathbf{a}(\phi)^H\ddot{\mathbf{a}}(\phi)\right\}\rho\alpha_{k,2p}\alpha_{k,2p-1}, \quad (31)$$

where $\dot{\mathbf{a}}(\phi) = \frac{\partial}{\partial\phi}\mathbf{a}(\phi)$. In (30), $\nu_{k,2p}(.)$ is given by:

$$\nu_{k,2p}(\rho) = \frac{d_p^2\ \beta_{k,2p}}{\sqrt{\pi}} \int_{-\infty}^{+\infty} \frac{\lambda^2_{k,2p}(t,\rho)}{\delta_{k,2p}(t,\rho)}\ e^{-\frac{t^2}{4}}\, dt,$$

where $\lambda_{k,2p}(t,\rho)$ and $\delta_{k,2p}(t,\rho)$ are displayed on the bottom of the current page. Now, after injecting the expectations evaluated in (29) to (31) back into (27), it can be shown that:

$$\gamma_{k,2p}(\phi) = 2\rho^2\big|\mathbf{a}(\phi)^H\dot{\mathbf{a}}(\phi)\big|^2\big[\nu_{2p}(\rho) - \omega_{k,2p}\big] + 2\rho\big\|\dot{\mathbf{a}}(\phi)\big\|^2\nu_{2p}(\rho) + 2\rho\Im\big\{\mathbf{a}(\phi)^H\ddot{\mathbf{a}}(\phi)\big\}\alpha_{k,2p}\alpha_{k,2p-1}.$$

By using equivalent algebraic manipulations, the other term $\gamma_{k,2p-1}(\phi)$ is obtained as:

$$\gamma_{k,2p-1}(\phi) = 2\rho^2\big|\mathbf{a}(\phi)^H\dot{\mathbf{a}}(\phi)\big|^2\big[\nu_{2p-1}(\rho) - \omega_{k,2p-1}\big] + 2\rho\big\|\dot{\mathbf{a}}(\phi)\big\|^2\nu_{2p-1}(\rho) - 2\rho\Im\big\{\mathbf{a}(\phi)^H\ddot{\mathbf{a}}(\phi)\big\}\alpha_{k,2p}\alpha_{k,2p-1}.$$

Finally, using the expressions of $\gamma_{k,2p}(\phi)$ and $\gamma_{k,2p-1}(\phi)$ in (26) and recalling (2), we obtain the closed-form expression of the DOA CA CRLB. Interestingly enough, this analytical expression is valid for any antenna array geometry. Yet, uniform linear arrays (ULAs) and uniform circular arrays (UCAs) remain by far the most studied cases in the open literature. For these two popular configurations, it can be shown (cf. [15]) that the required geometrical factors involved in $\gamma_{k,2p}(\phi)$ and $\gamma_{k,2p-1}(\phi)$ are given by[2]:

Table I. Geometrical factors for ULAs and UCAs

	ULA	UCA
$\big\|\dot{\mathbf{a}}(\theta)\big\|^2$	$\pi^2\,\frac{N_a(N_a-1)(2N_a-1)}{6}\cos^2(\theta)$	$\frac{N_a\pi^2}{8\sin^2(\pi/N_a)}$
$\lvert\mathbf{a}(\theta)^H\dot{\mathbf{a}}(\theta)\rvert^2$	$\pi^2\cos^2(\theta)\Big(\sum_{k=1}^{N_a-1}k\Big)^2$	0

[2]Note that the term $\Im\{\mathbf{a}(\phi)^H\ddot{\mathbf{a}}(\phi)\}$ cancels out by summing $\gamma_{k,2p}(\phi)$ and $\gamma_{k,2p-1}(\phi)$. For this reason, it is not included in Table I.

4. SIMULATION RESULTS

In this section, we illustrate the new DOA CA CRLB graphically with two modulation orders (i.e., 16− and 64−QAM), both with two coding rates ($R_1 = 1/2$ and $R_2 = 1/3$). In order to validate our new analytical expression, we also evaluated the considered bound empirically by following the same empirical approach used in [16] in the context of CA time delay estimation. As seen from Fig. 2, the new closed-form CRLB coincides with its *empirical* counterpart. It is also seen that, at the same SNR level and with the same coding rate, the CA CRLB increases as the modulation order increases. Moreover, at all SNR levels, the CA CRLB is smaller than the NDA CRLB, which corresponds to the case where all the symbols are completely unknown. This highlights the performance improvements in DOA estimation that can be achieved by a coded system over an uncoded one. More interestingly, the CA CRLB decreases rapidly to reach the DA CRLB, which corresponds to an ideal scenario where all the transmitted symbols are perfectly known to the receiver. Moreover, from Fig. 2 we see that the CA CRLB improves by decreasing the coding rate. In fact, with smaller coding rates, more redundancy is introduced by the encoder so that the decoder is more likely able to correctly detect the transmitted bits thereby enhancing the estimation performance.

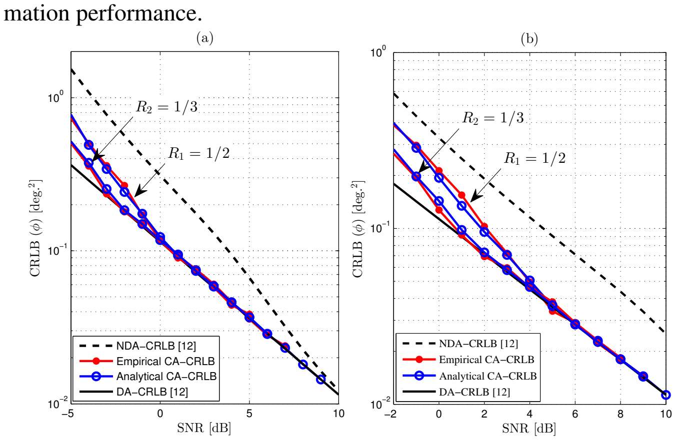

Fig. 2. Illustration of the DOA CA CRLBs for a ULA with $\phi = 45^\circ$ and $N_a = 4$: (a) 16−QAM ($K = 207$) and (b) 64−QAM ($K = 210$).

5. CONCLUSION

In this contribution, we established for the first time the closed-form expression for the CRLB of code-aided DOA estimates from turbo-coded square-QAM-modulated signals. The new expression was validated empirically by exhaustive Monte-Carlo simulations. It was shown that, by exploiting the turbo decoder output during the estimation process, the CA CRLBs become remarkably smaller than their NDA counterparts. This highlights the performance improvements that can be offered by coded systems, in terms of DOA estimation, as opposed to non-coded ones.

$$\lambda_{k,2p}(t,\rho) = \sum_{i=1}^{2^{p-1}} [2i-1]\theta_{k,2p}(i)\ e^{-\rho N_a d_p^2[2i-1]^2} \times \sinh\left(\sqrt{2\rho N_a}[2i-1]d_p t + \tfrac{L_{2p}(k)}{2}\right),$$

$$\delta_{k,2p}(t,\rho) = \sum_{i=1}^{2^{p-1}} \theta_{k,2p}(i) e^{-\rho N_a d_p^2[2i-1]^2} \times \cosh\left(\sqrt{2\rho N_a}[2i-1]d_p t + \tfrac{L_{2p}(k)}{2}\right).$$

6. REFERENCES

[1] H. Krim and M. Viberg, "Two decades of array signal processing research: the parametric approach," *Signal Process. Magazine,* vol. 52, no. 4, pp. 67-94, Jul. 1996.

[2] V. Lottici and M. Luise, "Embedding carrier phase recovery into iterative decoding of turbo-coded linear modulations," *IEEE Trans. Commun.,* vol. 52, no. 4, pp. 661-669, Apr. 2004.

[3] K. Choi, "Residual frequency offset compensation-embedded turbo decoder," *IEEE Trans. Veh. Technol.,* vol. 57, no. 5, pp. 3211-3217, May 2008.

[4] N. Noels, H. Steendam, and M. Moeneclaey, "The Cramér-rao bound for phase estimation from coded linearly modulated signals," *IEEE Commun. Lett.,* vol. 7, no. 5, pp. 207-209, May 2003.

[5] C. Morlet, I. Buret, and M.L. Boucheret, "A carrier phase estimator for multi-media satellite payloads suited to RSC coding schemes," in *Proc. of IEEE Int. Conf. Commun. (ICC),* vol. 1, New Orleans, LA, June 2000, pp. 455-459.

[6] C. Langlais and M. Helard, "Phase carrier recovery for turbo codes over a satellite link with the help of tentative decisions," in *Proc. of 2nd Int. Symp. Turbo Codes & Related Topics,* vol. 5, Sept. 2000, pp. 439-442.

[7] S. Cioni , G. E. Corazza, and A. Vanelli-Coralli, "Turbo embedded estimation with imperfect phase/frequency recovery," in *Proc. of IEEE Int. Conf. Commun.,* Anchorage, AK, June. 2003, pp. 2385-2389.

[8] W. Oh and K. Cheun, "Joint decoding and carrier phase recovery algorithm for turbo codes," *IEEE Commun. Lett.,* vol. 5, pp. 375-377, Sept. 2001.

[9] X. Wu, Y. Song, C. Zhao, and X. You, "Progressive frequency offset compensation in turbo receivers," *IEEE Trans. Wirel. Commun.,* vol. 10, no. 2, pp. 702-709, Fev. 2011.

[10] C. Berrou and A. Glavieux, "Near optimum error correcting coding and decoding: turbo codes," *IEEE Trans. Commun.,* vol. 44, no. 10, pp. 1261-1271, Oct. 1996.

[11] 3GPP TS 36.211: 3rd Generation Partnership Project; Technical Specification Group Radio Access Network; Evolved Universal Terrestrial Radio Access (E-UTRA); Physical Channels and Modulation.

[12] F. Bellili, S. Ben Hassen, S. Affès and A. Stéphenne, "Cramér-rao lower bounds of DOA estimates from square QAM-modulated signals," *IEEE Trans. Commun.,*, vol. 59, no. 6, pp. 1675-1685, June 2011.

[13] F. Bellili, S. Ben Hassen, S. Affès and A. Stéphenne, "Cramér-Rao bound for NDA DOA estimates of square QAM-modulated signals," in *Proc. of IEEE GLOBECOM'11*, Honolulu, HI, USA, Nov. 2009.

[14] S. M. Kay, *Fundamentals of statistical signal processing, vol. 1: Estimation theory*. Englewood Cliffs, NJ: Prentice-Hall, 1998.

[15] F. Bellili, S. Affes, and A. Stéphenne, "On the lower performance bounds for DOA estimators from linearly modulated signals," in *Proc. 25th Biennial Symposium Commun.*, May 2010.

[16] N. Noels, H. Wymeersch, H. Steendam, and M. Moeneclaey, "True cramér-rao bound for timing recovery from a bandlimited linearly modulated waveform with unknown carrier phase and frequency," *IEEE Trans. Commun.,* vol. 52, no. 3, pp. 473-483, Mar. 2004.

[17] F. Bellili, A. Methenni and S. Affès, "Closed-form CRLBs for SNR estimation from turbo-coded BPSK-, MSK-, and square-QAM-modulated signals," *IEEE Trans. Commun.,*, vol. 62, no. 15, pp. 4018-4033, Aug. 2014.

[18] F. Bellili, A. Methenni and S. Affès, "Closed-form CRLBs for CFO and phase estimation from turbo-coded square-QAM-modulated transmissions," accepted for publication in *IEEE Trans. Wirel. Commun.,* DOI 10.1109/TWC.2014.2387855, to appear.